

Radiation Characterization of Commercial GaN Devices

Richard D. Harris, *Member IEEE*, Leif Z. Scheick, *Member IEEE*, James P. Hoffman, *Member IEEE*, Tushar Thrivikraman, *Member IEEE* Masud Jenabi, Yonggyu Gim, and Tetsuo Miyahira

Abstract—Commercially available devices fabricated from GaN are beginning to appear from a number of different suppliers. In this initial study of the radiation tolerance of commercial GaN devices, several device types from several suppliers were chosen. Three different studies were performed: 1) a preliminary DDD/TID test of a variety of part types was performed by irradiating with 55 MeV protons, 2) a detailed DDD/TID study of one particular part type was performed by irradiating with 55 MeV protons, and 3) a SEB/SEGR test was performed on a variety of part types by irradiating with heavy ions. No significant degradation was observed in any of the tests performed in this study.

I. INTRODUCTION

GaN is a wide bandgap semiconductor material that has received considerable interest in recent years. There are a number of potential applications being explored, including high temperature ($>500^{\circ}\text{C}$), high power, and RF frequency devices. Commercial devices fabricated from GaN are beginning to appear from a number of different suppliers. Based on previous materials and prototype device studies [1]–[5], it is expected that these commercial devices will be quite tolerant to the types of radiation encountered in space. This expectation needs to be verified and the study described herein was undertaken for that purpose.

Most of the commercial GaN devices available today are fabricated in a HEMT structure. A typical structure of a GaN HEMT device is depicted in Fig. 1. The GaN material is epitaxially grown on a semi-insulating substrate. An AlGaIn layer is grown on top of the GaN and it is the AlGaIn/GaN interface that forms the active channel of the transistor.

The mismatch in the size of the bandgap of the two materials at the heterojunction interface results in the band structure depicted in Fig. 2. There is a conducting quantum well formed at the interface. Electronic conduction is via a 2 dimensional electron gas (2DEG) within this well. Because the conducting well is a natural consequence of the

heterojunction, the device is a normally on (depletion mode) device which requires a negative voltage to be applied to the gate to turn it off.

All parts discussed in this paper are readily available commercially. The parts chosen for study are all targeted for RF applications. They are all fabricated in the HEMT structure schematically depicted in Fig. 1.

II. EXPERIMENTAL DETAILS

The parts used in this study are summarized in Table I. Six different part types were chosen from three different suppliers. Also, a wide range of power capability was included.

Three separate tests were performed in this study: 1) a SEB/SEGR test was performed on a variety of part types by irradiating with heavy ions, 2) a preliminary DDD/TID test of a variety of part types was performed by irradiating with 55 MeV protons, 3) a detailed DDD/TID study of one particular part type was performed by irradiating with 55 MeV protons. Each of these three different tests will be described separately.

A. SEB/SEGR

The SEB/SEGR irradiations were carried out at Texas A&M University. The test ions were krypton at 953 MeV and xenon at 2530 MeV, 738 MeV, 522 MeV, and 391 MeV. The irradiations were done in air.

Measurements were made with a HP4142 Modular DC Source/Monitor. The NASA SEGR testing guideline (JPL Publication 08-10 2/08, “Testing Guideline for Single Event Gate Rupture (SEGR) of Power MOSFETs” [6]) was used as the testing standard.

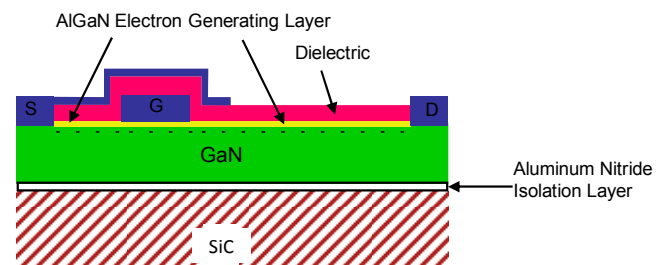


Fig. 1 Typical structure of a GaN HEMT device.

Manuscript received August 5, 2011. This work was carried out at the Jet Propulsion Laboratory, California Institute of Technology, Pasadena CA, under contract with the National Aeronautics and Space Administration (NASA). Support was provided by the NASA Electronic Parts and Packaging (NEPP) Program, the Deformation, Ecosystem Structure and Dynamics of Ice (DESDynI) mission, and the Jupiter Europa Orbiter (JEO) Mission.

The authors are with the Jet Propulsion Laboratory, California Institute of Technology, Pasadena, CA 91109 USA (richard.d.harris@jpl.nasa.gov, (phone: 818-393-6872, fax: 818-393-4559)).

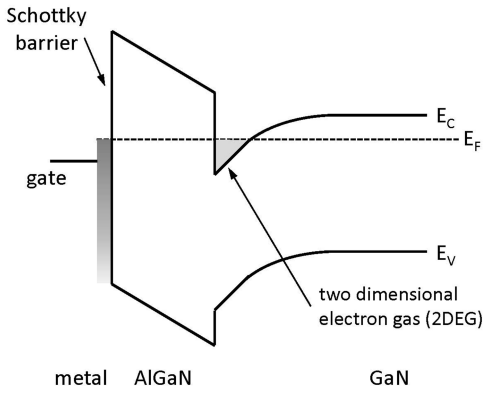


Fig. 2 Bandgap of a GaN HEMT structure at the heterojunction interface.

Since these devices have a lateral geometry, multiple angles were used to investigate any possible angular dependence. Also, various ion energies were used to ensure that any sensitive volume was struck. An HP4142 SMU provided the power supply and current monitoring to the test fixture and was controlled locally through a GPIB connection. This system has a time resolution for the measurements of ~ 100 ms and a current resolution of the SMU of 1 nA. During irradiation, the current through the gate, source, and drain pins was monitored while at a constant gate-to-source voltage (V_{GS}) and a constant drain-to-source voltage (V_{DS}). Between irradiations, a post irradiation gate stress (PIGS) test was done to screen for damage. If the DUT showed no damage, i.e., no shift in measured parameters, the voltage was incremented and re-irradiated.

B. Proton Irradiation

Parts were irradiated with protons to explore their potential sensitivity to displacement damage and ionizing damage as both are present during the exposure to high energy protons. Irradiations were carried out at the UC Davis Crocker National Laboratory (CNL) with 55 MeV protons from their cyclotron.

Two separate proton tests were carried out during the present study. A preliminary study was done which included a number of different part types; including all types in Table I for which proton irradiations are indicated. During this study only DC parameters were measured as the irradiation

progressed. Later, a more detailed study was performed in which only one part type was irradiated, but during which DC and RF parameters were measured.

1. Preliminary Test

For the preliminary test, proton fluences up to 1.6×10^{12} p/cm² were employed. Parts were irradiated in groups of 4 or 5 identical parts to provide information on part-to-part variability. As this irradiation progressed, two DC parametric measurements were made. First was the transfer characteristic (I_D vs. V_{GS} for various V_{DS}) which permitted the determination of the threshold voltage (V_{TH}). This measurement was made using an HP4156 Semiconductor Parameter Analyzer. The second measurement was the output characteristics (I_D vs. V_{DS} for various V_{GS}). This measurement was made with a Tektronix 370B High-Power Curve Tracer.

2. Detailed Test

For the detailed test, only the Cree 120 W parts were studied. Three parts were irradiated to a fluence of 1×10^{13} p/cm² and a fourth was continued to 1×10^{14} p/cm². As this irradiation progressed, the transfer characteristic, the output characteristic, and the RF power were measured.

All measurements were made with the parts soldered to a custom board shown in Fig. 3. This board was designed for the RF measurements. The measurement circuit is depicted in Fig. 4. The DC measurements were made by monitoring the drain and gate voltages from the power supply and the voltages across two precision resistors for the currents, with no RF power applied.

III. EXPERIMENTAL RESULTS

A. SEB/SEGR

There were no deleterious effects observed during the SEB/SEGR test. The parts revealed a very high leakage current ($> 1 \mu A$) during normal operation prior to applying the beam. As a result, the current injected by the heavy ion beam is small compared to the leakage current. This precludes there being any SEB effect. Similarly, no transient noise was observed. Again, this is explained since the leakage current is high compared to the injected charge. Similar results were observed for all ions and energies, all incident angles, and all parts.

TABLE I
SUMMARY OF PARTS TESTED

Supplier	P/N	Power Level (W)	Operating V_{DS} (V)	Date Code	Rad Tests Performed
Cree	CGH40010FE	10	28	14609, 22209	SEB/SEGR, Proton
	CGH40025FE	25	28	16509	Proton
	CGH40120FE	120	28	02310	SEB/SEGR, Proton
Sumitomo	EGB010MK	20	50		SEB/SEGR, Proton
	EGB045MK	90	50	30RY, 30SM	SEB/SEGR
RFMD	RF3934200	120	48		SEB/SEGR

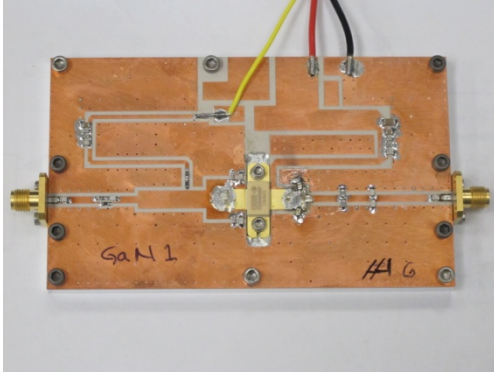


Fig. 3 Custom RF board used for the detailed irradiation of Cree 120W GaN parts.

B. Proton Irradiation

1. Preliminary Test

a. Threshold Voltage

A representative example of a transfer characteristic is shown in Fig. 5 for one of the Sumitomo parts. The drain/source voltage was set to 10 V and the gate/source voltage was swept from -3 to -1 V. Only the portion near the turn-on is shown to better show the threshold voltage. Similar data was also collected for $V_{DS} = 5, 8$ and 12 V and similar results were observed.

The transition from the off-state to the on-state is very abrupt. The steps used for the gate/source voltage in Fig. 5 were 5 mV and there are no points on the section of the curve between the off-state and the on-state. For subsequent plotting, the threshold voltage is taken to be the voltage of the last point in the off-state.

A plot of the threshold voltage vs. proton fluence is shown in Fig. 6 for the four different Sumitomo parts irradiated. There appears to be a small decrease in the threshold voltage for the lower fluence levels, but then no change for 2 parts and an increase for the other 2 parts for higher fluences. All-in-all, this is taken as an indication that there is at most a small change in V_{TH} with fluence and likely no real change.

The Cree parts showed similar behavior with the values moving around some, but again with no unambiguous trend. The Cree 120 W parts will be discussed later.

b. Output Characteristics

A representative example of the output characteristic is shown in Fig. 7 for a 25 W Cree part. The gate/source voltage

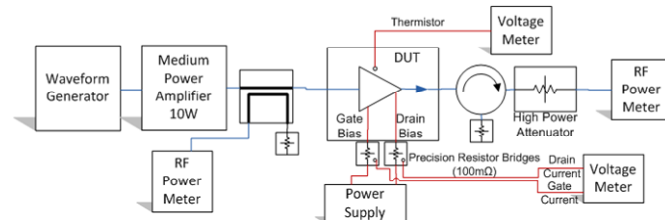


Fig. 4 Custom circuit used for the detailed irradiation of Cree 120W GaN parts.

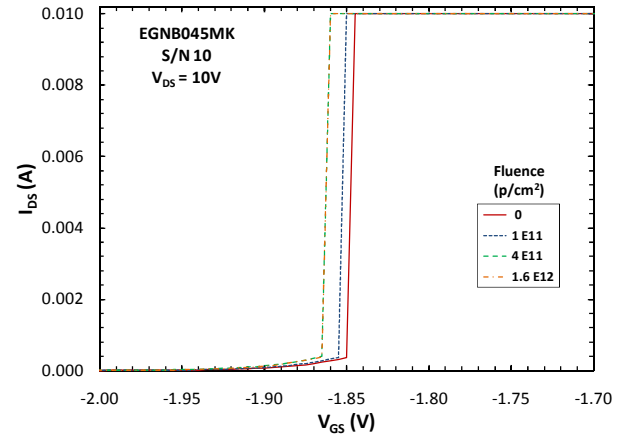


Fig. 5 Representative example of the transfer characteristic for a 45 W Sumitomo part as measured at $V_{DS} = 10$ V with a HP4156 Semiconductor Parameter Analyzer for several different fluences.

was set and the drain/source voltage was swept from 0 V until saturation appeared to be reached. Similar data was also collected for other gate voltages and similar results were observed; only 2 gate voltages are shown to avoid clutter on the graph. Five parts of this part number were irradiated and all showed similar behavior.

The curves following different levels of proton irradiation are all very similar. In addition, the small amount of variability that is observed shows no clear trend with increasing fluence. As a result, it appears that the proton irradiation has had no significant effect on the output characteristics.

The Sumitomo parts showed similar behavior with the values moving around some, but with no unambiguous trend.

2. Detailed Test

a. Threshold Voltage

A representative example of a transfer characteristic is shown in Fig. 8 for one of the Cree 120 W parts. The drain/source voltage was set to 28 V and the gate/source voltage was swept.

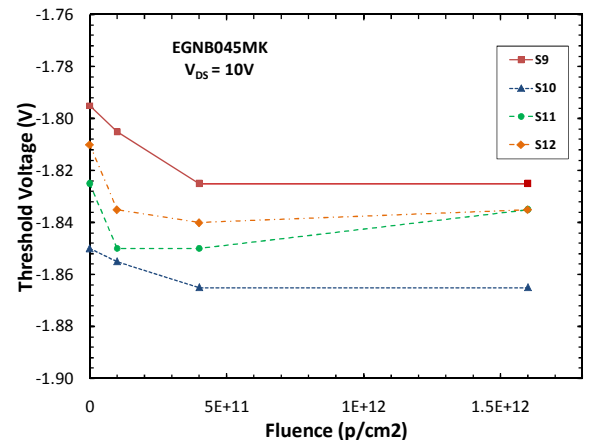


Fig. 6 Threshold voltage, V_{TH} , vs. fluence for the Sumitomo 45 W parts.

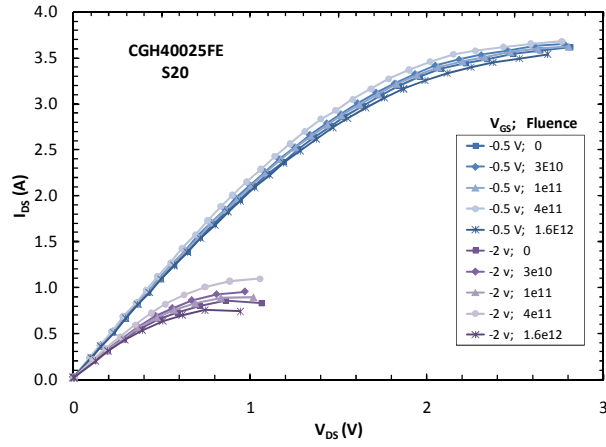


Fig. 7 Representative example of the output characteristics for a 25 W Cree part as measured with a Tektronix 370B High Power Curve Tracer for two values of V_G and several different proton fluences.

For this part and this measurement scheme, the transition from the off-state to the on-state is not as abrupt as seen previously. The linear region of the transfer curve at each fluence was extrapolated back to $I_D = 0$ A to give a value for the threshold voltage. A plot of threshold voltage vs. fluence for this part and the other parts is shown in Fig. 9. Values for a control sample are also included.

Both the irradiated samples and the control show some variation as the irradiation increases. However, there is no clear trend and the variation is small. As a result, there does not appear to be any significant change in V_{TH} . It is noted that the fluence is considerably higher in this test than the preliminary test. It is unlikely that any NASA missions are likely to exceed this level.

b. Output Characteristics

A representative example of the output characteristic is shown in Fig. 10 for one of the Cree 120 W parts for two different gate voltages. Data was recorded at other gate voltages with similar behavior.

The shape of the output characteristic is a bit unusual with

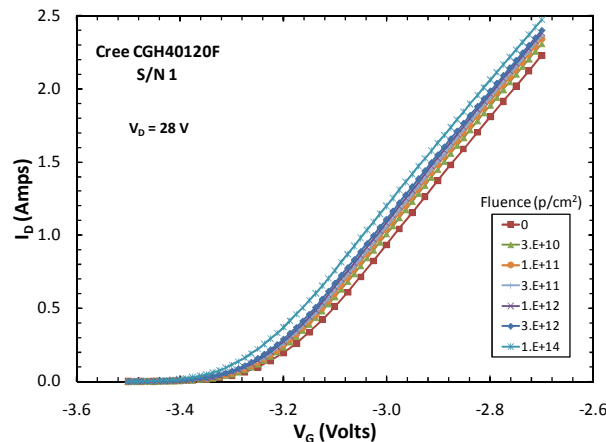


Fig. 8 Representative example of the transfer characteristic for a 120 W Cree part as measured at $V_{DS} = 28$ V for several different fluences.

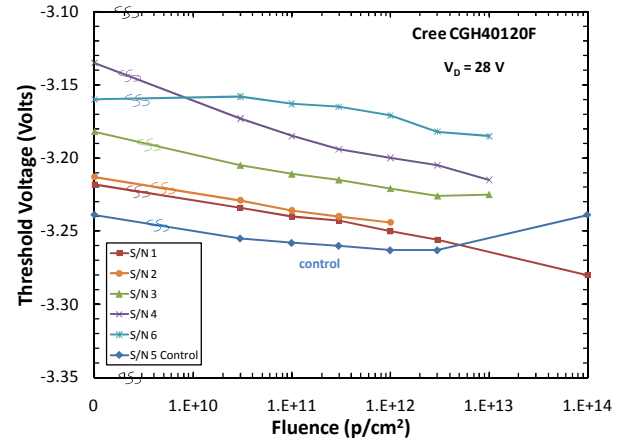


Fig. 9 Threshold voltage, V_{TH} , vs. fluence for the 120 W Cree part as measured at $V_{DS} = 28$ V.

the current decreasing at higher drain voltages. This is attributed to a phenomenon known as dispersion that results from charge accumulating on the top of the device dielectric material adjacent to the gate electrode [7]. It is possible to passivate this charge by using a suitable cap material on top of the dielectric [7]. Apparently Cree has chosen to not use such a cap on these devices at this time.

A plot of the output current at $V_D = 35$ V vs. fluence is shown in Fig. 11 for the two different gate voltages. Very little change is observed as the fluence increases. As a result, there does not appear to be any significant change in output current due to the irradiation.

c. RF Power

A representative example of power-in vs. power-out is shown in Fig. 12 for one of the Cree 120 W parts as measured at 1.22 GHz. A linear relationship between P_{IN} and P_{OUT} is observed.

A plot of the output power vs. fluence is shown in Fig. 13. Values measured on the control sample are also shown. Very little change is observed as the fluence increases. As a result, there does not appear to be any significant change in output current due to the irradiation.

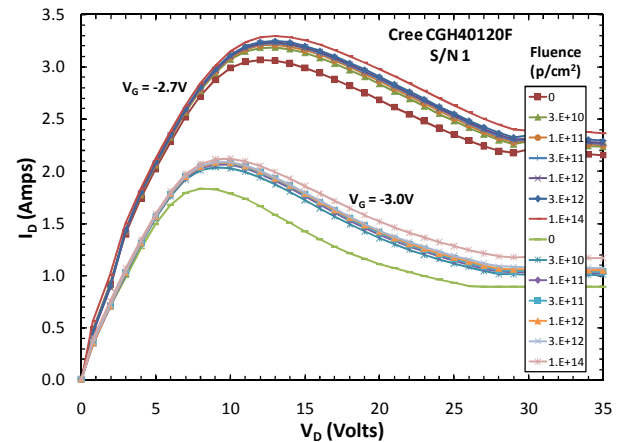


Fig. 10 Representative example of the output characteristic for a 120 W Cree part as measured at two different gate voltages for several different fluences.

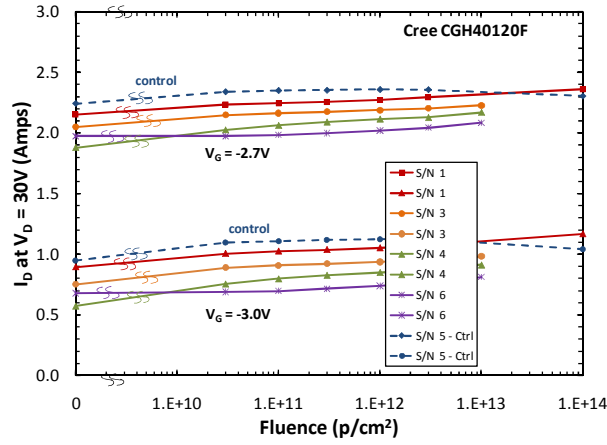


Fig. 11 Output current, I_D , vs. fluence for the 120 W Cree part for $V_D = 35$ V as measured at $V_{GS} = -1.7$ V and -3.1 V.

IV. DISCUSSION

The GaN HEMT devices reported in this study show no significant amount of degradation for the irradiations discussed in this paper. There is no indication of SEGR or SEB with heavy ion irradiation. There is no indication of significant parameter degradation following proton irradiation.

These results can be explained through an understanding of the device structure shown in Fig. 1. The gate on a HEMT device is a Schottky junction and not an oxide. As a result, there is no possibility of gate rupture. Also, because of the

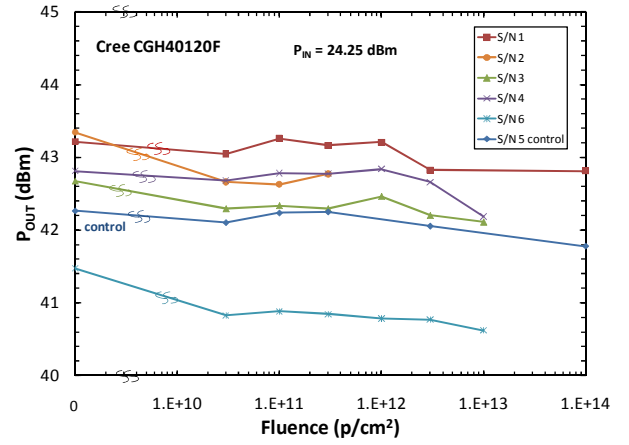


Fig. 13 Output power vs. fluence for the 120 W Cree part with $P_{IN} = 10.27$ dBm.

junction at the gate, the leakage current is very high. The current injected by an ion strike is small compared to this leakage current and is insufficient to induce an SEB event.

There is no oxide or other insulator at the gate or anywhere else in the structure. Therefore no TID degradation would be expected.

It is expected that there will be DDD effects in this structure if the irradiation is carried out to sufficiently high levels. The fluence used in this study, 1×10^{14} p/cm² (50 MeV), is a fairly high level for displacement damage for NASA missions. It will be left to future work to carry the proton irradiation to more extreme levels in order to determine the level at which DD effects begin.

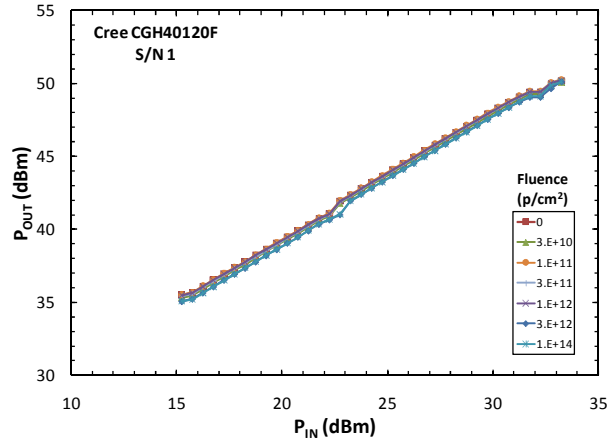


Fig. 12 Representative example of the power-in vs. power-out for output characteristic for a 120 W Cree part as measured at 1.22 GHz for several different fluences.

V. REFERENCES

- [1] A.H. Johnson, Reliability and Radiation Effects in Compound Semiconductors, New Jersey, World Scientific, 2010.
- [2] A. Ionascut-Nedelcescu, et. al., "Radiation hardness of gallium nitride", IEEE Trans. Nucl. Sci., vol 49, no. 6, pp. 2733 – 2738, Dec. 2002.
- [3] P.J. Sellin and J. Vaitkus, "New materials for radiation hard semiconductor detectors", Nucl. Inst. Meth. Phys. Res., Vol. 557, pp. 479-489, 2006.
- [4] X Hu, et. al., "Proton-irradiation effects on AlGaIn/GaN high electron mobility transistors", IEEE Trans. Nucl. Sci., vol 50, no. 6, pp. 1791 – 1796, Dec. 2003.
- [5] O. Aktas, et. al., "60Co gamma radiation effects on DC, RF, and pulsed I-V characteristics of AlGaIn/GaN HEMTs," Sol.-St. Elect., Vol. 48, pp. 471-475, 2004.
- [6] L.Z. Scheick, "Testing Guideline for Single Event Gate Rupture (SEGR) of Power MOSFETs", JPL Publication 08-10, 2008.
- [7] L. Shen, R. Coffie, D. Buttari, S. Heikman, A. Chakrakorty, A. Chini, S. Keller, S.P. Denbaars, and U.K. Mishra, "Unpassivated GaN/AlGaIn/GaN power high electron mobility transistors with dispersion controlled by epitaxial layer design", J. Elect. Mat. Vol. 33, pp. 422-425, 2004.